Nonsmooth Bifurcations in a Piecewise-Linear Model of the Colpitts Oscillator

Gian Mario Maggio, *Member IEEE*, Mario di Bernardo, *Associate Member, IEEE*, and Michael Peter Kennedy, *Fellow, IEEE*

***Abstract*—This paper deals with the implications of considering a first-order approximation of the circuit nonlinearities in circuit simulation and design. The Colpitts oscillator is taken as a case study and the occurrence of discontinuous bifurcations, namely, border-collision bifurcations, in a piecewise-linear model of the oscillator is discussed. In particular, we explain the mechanism responsible for the dramatic changes of dynamical behavior exhibited by this model when one or more of the circuit parameters are varied. Moreover, it is shown how an approximate one-dimensional (1-D) map for the Colpitts oscillator can be exploited for predicting border-collision bifurcations. It turns out that at a border-collision bifurcation, a 1-D return map of the Colpitts oscillator exhibits a square-root-like singularity. Finally, through the 1-D map, a two-parameter bifurcation analysis is carried out and the relationships are pointed out between border-collision bifurcations and the conventional bifurcations occurring in smooth systems.**

***Index Terms*—Border-collision bifurcations, Colpitts oscillator, grazing, nonsmooth systems, one-dimensional map, sliding mode.**

I. Introduction

THE AIM of this paper is to highlight the occurrence of nonsmooth bifurcations in piecewise-linear (PWL) circuits and to provide the designer with some practical tools to deal with these phenomena. By nonsmooth bifurcations, we mean here the characteristic bifurcations taking place in nonsmooth systems (that is, characterized by at least one discontinuity in the vector field or its derivatives) that cannot occur in smooth systems. The motivation for this paper comes from the common engineering practice of using a first-order approximation of the circuit nonlinearities for circuit simulation and design purposes [1], [2].

A great research effort has been devoted in the last few years to investigate the dynamics of PWL circuits [3]–[7]. The main advantage of considering PWL models is that analytical methods can be applied for a bifurcation analysis of the system. Namely, we will use techniques developed for the analysis of generic piecewise-smooth (PWS) systems [8]. These analytical tools have also been shown to be particularly effective in explaining the dynamics exhibited by electronic circuits such as power electronic dc/dc converters [9]–[12].

In this paper we consider the Colpitts oscillator as a case study for its relevance in applications and for the richness of its dynamical behavior. The Colpitts oscillator is one of the most widely used single-transistor circuits to produce sinusoidal oscillations at radio frequencies. Recently, both numerical and experimental evidence has been reported of the occurrence of nonlinear phenomena such as bifurcations and chaos in this circuit [13]–[17].

We will attempt to explain the complex dynamics exhibited by the Colpitts oscillator by studying the nonsmooth bifurcations of a PWL model of the circuit. This novel approach can be easily integrated with the analysis of the smooth model of the Colpitts oscillator presented in [17]. The goal is to point out differences and similarities in the behavior when considering a nonsmooth model versus a smooth one.

The PWL model that we will consider is an instance of a wider class of PWS systems characterized by a change of configuration whenever a linear combination of the system states satisfies a given constraint. The state space of these systems can then be divided into different regions associated with the different smooth-system configurations. We will assume that, on the boundaries between different regions, the flow of the system is continuous, but has a discontinuous first derivative (nonsmooth). In this case, the so-called *border-collision* or C*-bifurcation* [18], [19], has been shown to occur when a system solution becomes tangent to one of the state-space boundaries, as the system parameters are varied. We remark that this definition is rather general and can be applied to both continuous-time and discrete-time systems of arbitrary dimension [8], [20]. In particular, the "singular bifurcation into instant chaos" first described in [5] can be considered as a particular case of border-collision bifurcation.

In what follows, we will outline the important role played by border-collision bifurcations in organizing the dynamical behavior of our model of the Colpitts oscillator. Moreover, by using the technique introduced by Feigin in [19], we will show how to carry out a classification of the possible border-collision bifurcations exhibited by the circuit. Also, we will outline the use of a one-dimensional (1-D) approximate map to further analyze the occurrence of these nonsmooth phenomena.

The rest of the paper is organized as follows. After introducing the system model in Section II and illustrating its dynamical behavior in Section III, an overview of nonsmooth bifurcations in PWS systems is presented in Section IV. The an-

Manuscript received October 23, 1998; revised October 29, 1999 and March 9, 2000. This paper was recommended by Associate Editor, H. Kawakami. The work of G. M. Maggio and M. P. Kennedy was supported by the TMR program, the European Union, under Grant ERBFMBICT950310 and by the Forbairt International Collaboration Grant IC/98/052. The work of M. di Bernardo was supported by the Nuffield Foundation (NUF-NAL scheme) and the Institute under Project 99-1-02. This paper was recommended by Associate Editor H. Kawakami.

G. M. Maggio is with the Institute for Nonlinear Science (INLS), University of California, San Diego, La Jolla, CA 92093-0402 USA (e-mail: gmaggio@ucsd.edu).

M. di Bernardo is with the Department of Engineering Mathematics, University of Bristol, Bristol, U.K. (e-mail: M.diBernardo@bristol.ac.uk).

M. P. Kennedy is with the Department of Microelectronic Engineering, University College Cork, Cork, Ireland (e-mail: Peter.Kennedy@ucc.ie).

Publisher Item Identifier S 1057-7122(00)06329-7.

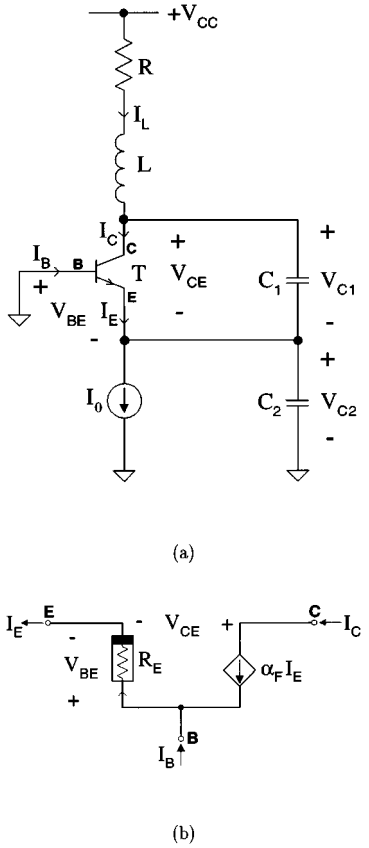

Fig. 1. Circuit model. (a) Schematic of the Colpitts oscillator. (b) Transistor model in common-base configuration.

alytical and numerical study of border-collision bifurcations in the Colpitts oscillator is then presented in Section V. Finally, in Section VI, an approximate 1-D map for the Colpitts oscillator is introduced and employed to carry out a bifurcation analysis of the system under investigation.

II. Circuit Model

A. State Equations

We consider the classical schematic for the Colpitts oscillator containing a bipolar junction transistor (BJT) as the gain element and a resonant network consisting of an inductor and a pair of capacitors, as illustrated in Fig. 1(a). The transistor T, in common-base configuration, is modeled as shown in Fig. 1(b), i.e., by a (voltage-controlled) nonlinear resistor R_E and a linear current-controlled current source, namely $I_C = \alpha_F I_E$, where α_F is the common-base forward short-circuit current gain.

The state equations for the schematic in Fig. 1(a) are as follows:

$$\begin{aligned} C_1 \frac{dV_{C_1}}{dt} &= -\alpha_F f(-V_{C_2}) + I_L \\ C_2 \frac{dV_{C_2}}{dt} &= (1-\alpha_F) f(-V_{C_2}) + I_L - I_0 \\ L \frac{dI_L}{dt} &= -V_{C_1} - V_{C_2} - RI_L + V_{CC} \end{aligned} \tag{1}$$

where (V_{C_1}, V_{C_2}, I_L) are the circuit-state variables and $f(\cdot)$ is the driving-point characteristic of the nonlinear resistor. This characteristic can be expressed in the form $I_E = f(V_{BE}) = f(-V_{C2})$, which we model by a PWL relation, namely

$$I_E = \begin{cases} I_0 \left(\dfrac{V_{BE} - V_{\rm th}}{V_T} \right), & V_{BE} \geq V_{\rm th} \quad \text{(forward active)} \\ 0, & V_{BE} < V_{\rm th} \quad \text{(cutoff)} \end{cases}$$

where $V_{\rm th} = V_T[\ln(\alpha_F I_0/I_S) - 1]$ is the threshold voltage, I_S is the saturation current of the base-emitter junction, and $V_T \simeq 26$ mV at room temperature.

From (1), it follows also that the operating point O of the oscillator can be defined by

$$O: \begin{cases} V_{C_{10}} = V_{CC} - \alpha_F R I_0 + V_T \ln \left(\alpha_F \dfrac{I_0}{I_S} \right) \\ V_{C_{20}} = -V_T \ln \left(\alpha_F \dfrac{I_0}{I_S} \right) \\ I_{L_0} = \alpha_F I_0. \end{cases} \tag{2}$$

B. Normalization and Parameters

We now introduce a set of dimensionless state variables (x_1, x_2, x_3) by choosing the operating point O of (1) to be the origin of the new coordinate system and by normalizing voltages, currents, and time with respect to $V_{\rm ref} = V_T$, $I_{\rm ref} = I_0$, and $t_{\rm ref} = 1/\omega_0$, respectively, where

$$\omega_0 = \frac{1}{\sqrt{L \dfrac{C_1 C_2}{C_1 + C_2}}}$$

is the resonant frequency of the unloaded tank circuit. In particular, the following relations hold

$$\begin{aligned} x_1(t) &= \frac{1}{V_T} \left[V_{C_1}(\omega_0 t) - V_{C_{10}} \right] \\ x_2(t) &= \frac{1}{V_T} \left[V_{C_2}(\omega_0 t) - V_{C_{20}} \right] \\ x_3(t) &= \frac{1}{I_0} \left[I_L(\omega_0 t) - I_{L_0} \right] \end{aligned}$$

where $V_{C_{10}}$, $V_{C_{20}}$, and I_{L_0} are defined in (2).

By setting $\alpha_F = 1$ (which corresponds to neglecting the current flowing into the base of the BJT) the state equations (1) of the Colpitts oscillator can be rewritten in the form

$$\begin{pmatrix} \dot{x}_1 \\ \dot{x}_2 \\ \dot{x}_3 \end{pmatrix} = \begin{pmatrix} \dfrac{g}{Q(1-k)} [-n(x_2) + x_3] \\ \dfrac{g^*}{Qk} x_3 \\ -\dfrac{Qk(1-k)}{g^*} [x_1 + x_2] - \dfrac{1}{Q} x_3 \end{pmatrix} \tag{3}$$

where

$$n(x_2) = \begin{cases} -x_2, & x_2 \leq 1 \quad \text{(forward active)} \\ -1, & x_2 > 1 \quad \text{(cutoff)} \end{cases}$$

and $k = C_2/(C_1 + C_2)$. It follows that the PWL model of the Colpitts oscillator is discontinuous (C^0) on the plane $x_2 = 1$, corresponding to the boundary between the forward active and cutoff regions of operation of the BJT.

(a)

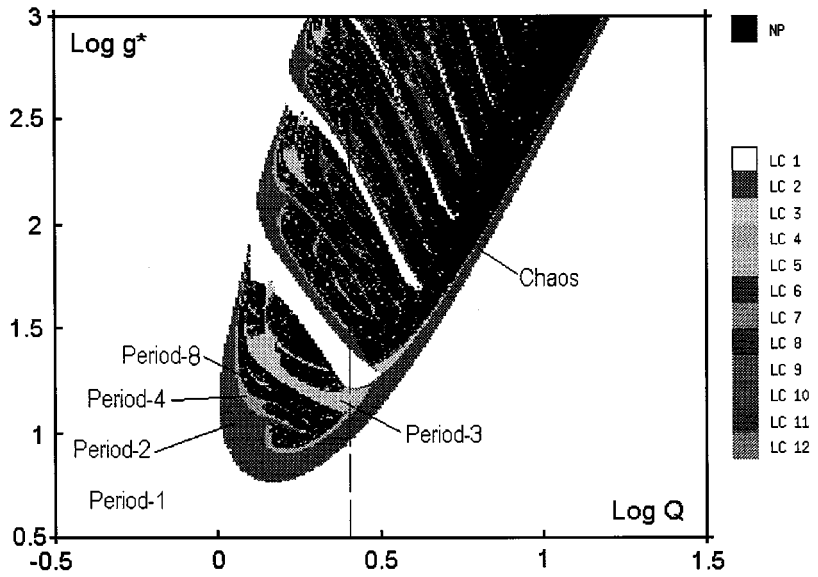

(b)

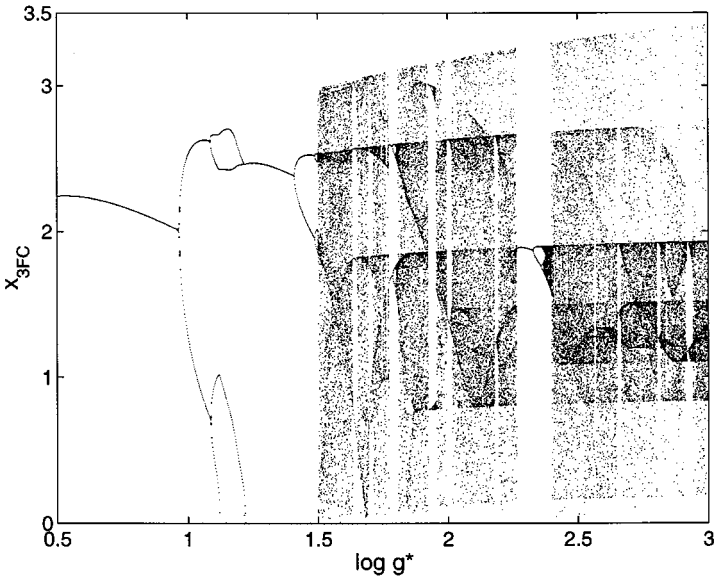

Fig. 2. Dynamical behavior of the Colpitts oscillator. (a) Two-parameter bifurcation diagram (by simulation); the characteristic "fish-hook" structures are visible. (b) One-parameter bifurcation diagram for $\log\ Q \simeq 0.4$, corresponding to the vertical line in (a); note that x_{3FC} is the value of the coordinate x_3 at the points of intersection of the system trajectory with the Poincaré section $x_2 = 1$, for $\dot{x}_2 > 0$, i.e., corresponding to the transition from the forward active (F) to the cutoff (C) region of operation of the BJT.

Finally, it should be noted that (3) depends only on the two parameters:

- $Q = ((\omega_0 L)/R)$, the quality factor of the (unloaded) tank circuit;
- g^*, the "loop gain" of the oscillator

while k has only a scaling effect on the state variables.

Also, note that g^* represents the value of the loop gain at which the phase condition of the Barkhausen criterion [21] is satisfied (for $\alpha_F = 1$). In particular, the oscillator will start oscillating only if the start-up condition $g^* > 1$ ($\Longleftrightarrow \log g^* > 0$) is fulfilled.

III. Observed Dynamical Behavior

The plethora of different dynamical behaviors exhibited by the Colpitts oscillator can be best summarized by looking at the system's bifurcation diagram. In particular, Fig. 2(a) shows a two-parameter bifurcation diagram (by simulation) illustrating the dependence of the dynamical behavior of the PWL model of the Colpitts oscillator on the two parameters Q and g^*. This bifurcation diagram has been obtained by numerical integration of the system (3) throughout the parameter space (Q, g^*). The resulting trajectories are analyzed[1] in order to establish whether the system, at steady state, settles to an equilibrium point, a limit cycle, or a chaotic attractor. Different behaviors are represented by different "colors" in the diagram. In Fig. 2(a), "LCn" indicates that the original system settles to a period-n limit cycle. For example "$LC1$" denotes the fundamental period-1 limit cycle, which corresponds to nearly sinusoidal oscillation of the

[1]The algorithm to determine the dynamical behavior of the system was implemented using the C-library CHAOSLIB by Abel and Wegener (e-mail: wegener@vdp.ucd.ie).

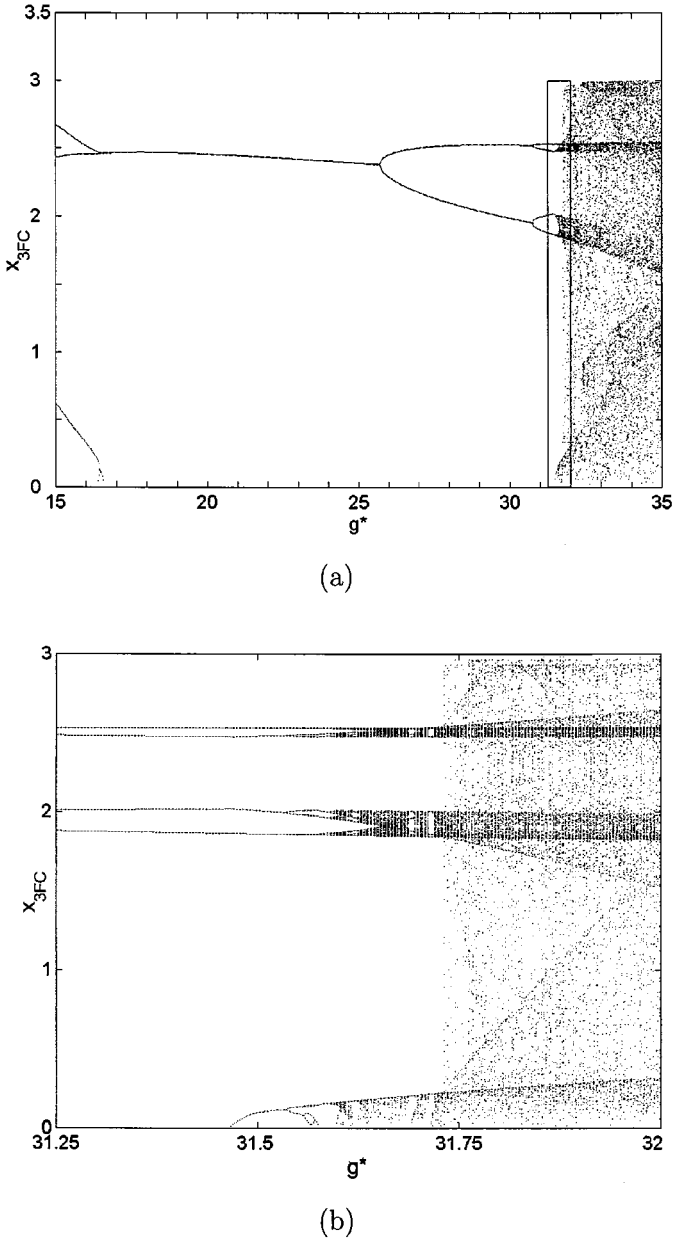

Fig. 3. (a) Detail of the bifurcation diagram for $Q = 2.5 (\log Q \simeq 0.4)$ in Fig. 2(b). Notice the sudden disappearance of one branch of the diagram at $g^* \approx 16.57$ and the occurrence of chaos at $g^* \approx 31.5$, as better visible in the zoom (b) of the boxed region in (a). Both of these phenomena are due to border-collision bifurcations and these correspond to the appearance of points close to $x_3 = 0$ on the bifurcation diagram.

Colpitts oscillator. Conversely, "NP" indicates that no periodic behavior was detected, and so we associate nonperiodic behavior with the corresponding region. We note the presence of a large region of complex behavior in the parameter space in which the system undergoes several bifurcations when varying either of the parameters Q or g^*. Also, it should be noted in Fig. 2(a) the presence of the characteristic "fish-hook" structures described for example in [22].

Fig. 2(b) shows the one-parameter bifurcation diagram corresponding to the vertical line at $\log Q \simeq 0.4$ in Fig. 2(a). This diagram is obtained by plotting the coordinate x_3 on the Poincaré section $x_2 = 1$ (with $\dot{x}_2 > 0$) when the parameter g^* is varied, for a fixed value of $Q(= 2.5)$. From Fig. 2(b), we can see that the system solution undergoes several bifurcations as the value of the "loop gain" g^* is increased. The observed bifurcation scenario, though, cannot be explained just as a sequence of smooth local bifurcations since several nonsmooth phenomena can be identified. For instance, in the zoom of the bifurcation diagram for $Q = 2.5$, reported in Fig. 3(a), we can observe a "jump" from a period-2 orbit onto a period-1 solution for $g^* \approx 16.5$. The resulting orbit then undergoes a few period doublings until the sudden occurrence of chaotic evolution at $g^* \approx 32$, as visible with more details in Fig. 3(b).

The explanation of these discontinuous phenomena will be the subject of the rest of this paper.

IV. Border Collision and Grazing Bifurcations

A. Overview

As briefly detailed in Section I, an important class of bifurcations for PWS systems are the so-called grazing and *border-collision bifurcations* (also termed C-bifurcations in the Russian literature) [18], [20], [23], [24]. Namely, consider a system of the form

$$\dot{x} = F(x, t, \mu) \tag{4}$$

with $x \in R^n$ being the state vector, $\mu \in R^p$ the parameter vector, and F: $R^{n\times 1\times p} \mapsto R^n$ a PWS function. The state space of such a system can be divided into countably many regions; in each region, the system has a different smooth functional form. At the boundaries of these regions, F can be either continuous or have a discontinuous first derivative (nonsmooth).

A *border-collision bifurcation* is said to occur when, by varying the system parameters, a system trajectory becomes tangent to one of these boundaries and the system flow is continuous, but nonsmooth, across them. If, instead, the flow is discontinuous, a *grazing* bifurcation takes place. In both cases, a consistent change in the dynamical evolution of the system is often detected [5], [6], [18], [19], [25]. Namely, after a border-collision, the following scenarios are usually observed.

1) A continuous transition from the orbit involved in the bifurcation to an orbit of a similar or different periodicity, which contains one or more trajectory sections in another region of the state space (i.e., the transition from a periodic orbit to one of a similar type having an additional section lying on the other side of the boundary or period doubling).
2) The merging of two different solutions (existing on both sides of a state space boundary), followed by their disappearance.
3) The sudden transition from a periodic orbit to chaotic evolution (see for example [5]).

Also, it has been shown [10], [11], [26] that when an orbit of the system becomes tangent to one of the state-space boundaries, the Jacobian of the corresponding Poincaré map (from the switching plane to itself) has a singularity. In particular, one of the eigenvalues of the Jacobian diverges to infinity, while the other approaches zero. Hence, *infinite local stretching* is introduced along one direction in the state space. This phenomenon has been shown to be the cause of many other interesting features induced by border-collision bifurcations such as, for instance, chaotic attractors characterized by fingered structures,

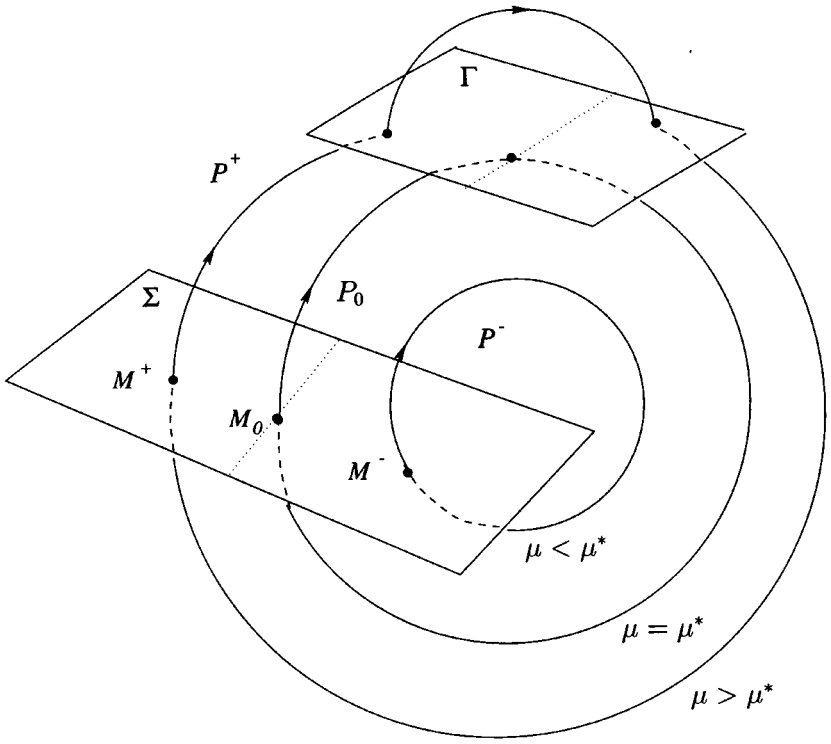

Fig. 4. Local analysis of a border-collision bifurcation. See the text for a detailed explanation.

period-adding cascades, hysteretic phenomena (due to switching between coexisting attractors), and sudden jumps to chaos.

Finally, it can be shown that while border collisions are characterized by PWL normal forms, grazing bifurcations are in contrast described by normal forms containing a square-root singularity. Nevertheless, we will show that, under certain conditions, border-collision bifurcations in the Colpitts oscillator are associated with square-root singularities of the appropriately derived 1-D map. This is an interesting result that seems to suggest an unexpected link between these two classes of bifurcation. More work in this direction will be published elsewhere.

B. Classification of Border-Collisions

An effective method to classify and predict the dynamical scenario following a border-collision bifurcation was introduced by the Russian scientist M. I. Feigin in the late 1970s. A desription of the method can be found in [19].

This method is based on the definition of an appropriate local map describing the system dynamics in a neighborhood of a border-collision bifurcation. The characterization of the bifurcation is then obtained by studying the eigenvalues of this local map. Namely, suppose that for a given parameter value, say μ^*, a periodic orbit P_0 of the system under investigation becomes tangent to one of the state-space boundaries Γ and let M_0 denote the corresponding fixed point on some appropriately chosen Poincaré section Σ (see Fig. 4). Assume also, without loss of generality, that by perturbing the system parameter in a neighborhood of μ^*, the system orbit P_0 does not touch the boundary if $\mu < \mu^*$, but crosses it if $\mu > \mu^*$. As the parameter varies, the fixed point M_0 associated with P_0 will move accordingly on Σ from the point M^- (associated with the orbit that does not cross the boundary) to the point M^+ (associated with the orbit

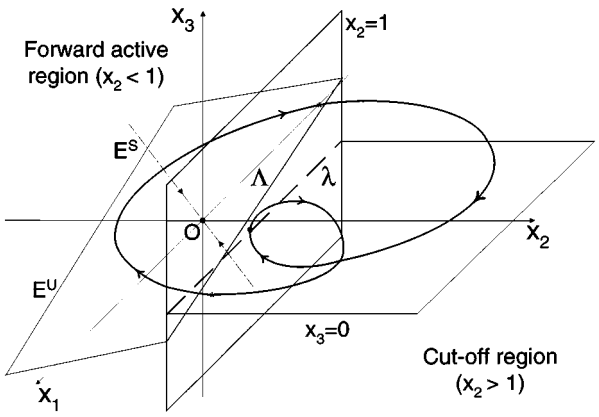

Fig. 5. State-space interpretation of a border-collision bifurcation. The stable (E^S) and unstable (E^U) eigenspaces associated with the equilibrium point at the origin are also shown.

that crosses the boundary). Notice that the Poincaré section Σ cannot be chosen to be the switching surface itself, since before the occurrence of the tangency $\mu < \mu^*$ the system orbit does not cross Σ and hence no fixed point M^- can be isolated.

Now, let J_m be the Jacobian matrix of the fixed point M^- on Σ for $\mu < \mu^*$. Similarly, denote by J_p the Jacobian of the fixed point M^+ on Σ corresponding to the system orbit which crosses the boundary for $\mu > \mu^*$. If we say σ_m^+, σ_p^+ the number of eigenvalues greater than 1 of J_m and J_p, respectively, and σ_m^-, σ_p^- the number of eigenvalues less than -1, we have, according to Feigin's method that, after a border-collision, an orbit of a given type:

1) smoothly changes into one containing an additional section in the other region of the state space if $\sigma_m^+ + \sigma_p^+$ is even;

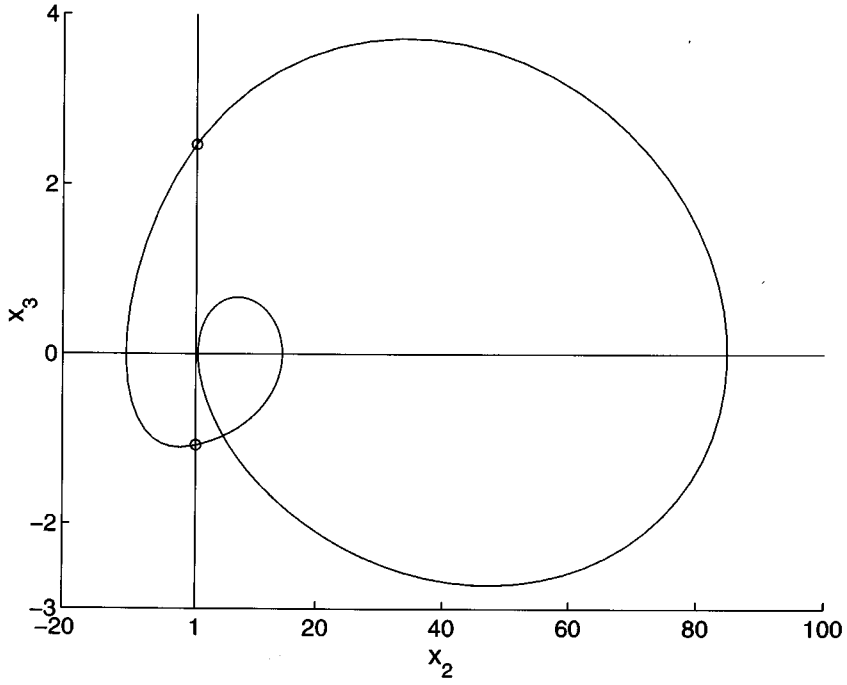

Fig. 6. Periodic orbit at $g^* = 16.8$. As g^* is decreased, the inner lobe approaches the switching surface $x_2 = 1$ tangentially, at $x_3 = 0$.

2) suddenly disappears after touching the boundary if $\sigma_m^+ + \sigma_p^+$ is odd;
3) undergoes a period doubling if $\sigma_m^- + \sigma_p^-$ is odd.

Notice that, as shown in [11] and [19], these three elementary conditions can be used to build bifurcation scenarios of increasing complexity which include the sudden jump to chaos outlined in the previous section.

An application of this method in the case of the Colpitts oscillator will be presented in Section V-B.

V. Border-Collision Bifurcations in the Colpitts Oscillator

The state space (x_1, x_2, x_3) associated with the PWL model of the Colpitts oscillator can be split into two regions, depending on the mode of operation of the BJT. In particular, for $x_2 < 1$ the transistor works in the forward active region, while for $x_2 > 1$ it is cutoff. Thus, as shown in Fig. 5, the surface $x_2 = 1$ can be seen as the boundary between the two different regions in state space associated with the two possible system configurations. Notice that this surface is defining a boundary between the two different regions in the state space corresponding to the two possible system configurations. Hence, we conjecture that, for the system under investigation, a border-collision bifurcation will take place whenever a part of the system trajectory becomes tangent to the plane $x_2 = 1$, i.e., $x_2 = 1$, $\dot{x}_2 = 0$. Notice from system (3) that the second equation is of the form

$$\frac{dx_2}{dt} \propto x_3.$$

Therefore, we can deduce that

$$\dot{x}_2 = 0 \iff x_3 = 0$$

and the conditions for a border-collision are then satisfied along the line λ (see Fig. 5) defined by

$$\lambda: \begin{cases} x_2 = 1 \\ x_3 = 0. \end{cases} \tag{5}$$

A. Numerical Evidence

For the sake of clarity, in this section we will refer to nonsmooth bifurcations occurring along the one-parameter bifurcation diagram depicted in Fig. 3(a), for $Q = 2.5$.

In what follows, we will investigate the occurrence of the following nonsmooth bifurcations (see Fig. 3):

- The abrupt interruption of one of the bifurcation diagram branches for $g^* \simeq 16.57$;
- The sudden "jump" to a chaotic evolution observed at $g^* \simeq 31.5$;
- The enlargement of a chaotic attractor observed for $g^* \simeq 31.75$.

Similar phenomena can also be found for other values of the parameter Q in the two-parameter bifurcation diagram depicted in Fig. 2(a). Detailed numerical simulations clearly show that these phenomena are due to the occurrence of tangencies between one of the periodic solutions and the switching surface $x_2 = 1$ (border-collisions).

The dynamical evolution of the system around $g^* \simeq 16.578$ is shown in Figs. 6 and 7. Starting from $g^* = 16.8$ and decreasing the parameter value, we see that the inner lobe of the periodic orbit shown in Fig. 6 becomes tangent to the switching surface (i.e., $x_2 = 1$, $\dot{x}_2 = x_3 = 0$) at $g^* = 16.578$ (border-collision). Then a smooth transition is observed to a new periodic orbit, shown in Fig. 7(a). This orbit is similar to the one involved in the border collision but is characterized by a new section lying on the other side of the state-space boundary; see Fig. 7(b). On the bifurcation diagram shown in Fig. 3(a), this dynamical transition

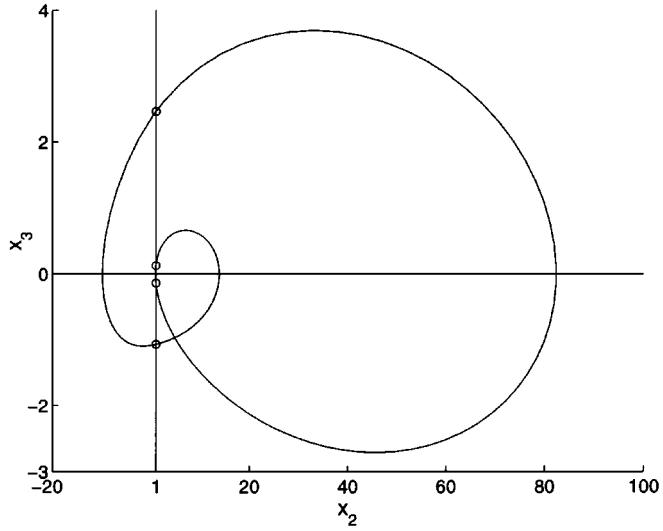

(a)

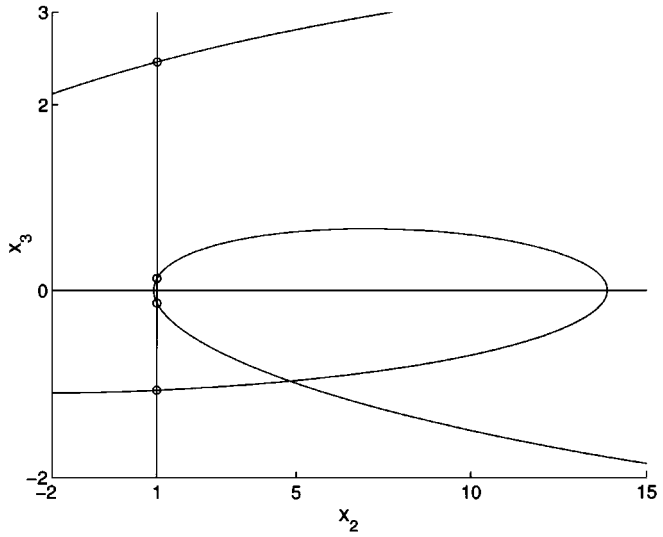

(b)

Fig. 7. (a) Periodic orbit at $g^* = 16.45$, immediately after the border-collision bifurcation. Note that the orbit is very similar to the one depicted in Fig. 6, but now its inner lobe (b) does not lie entirely within one of the state space regions.

corresponds to the sudden appearance of an additional bifurcation branch[2] for $g^* < 16.578$. A further numerical investigation indicates that at $g^* = 16.425$ the orbit generated at the border collision undergoes a classical period-doubling bifurcation.

From the bifurcation diagrams reported in Fig. 3(a) and (b), it is also evident that for $g^* = 31.5$ a classical period-doubling cascade is abruptly interrupted by a sudden transition from a periodic orbit to a chaotic evolution. The system state-space trajectories for these values of the parameters are reported in Fig. 8, where the situation immediately "before" and "after" the occurrence of the jump to chaos is shown. We can see that as g^* increases, the period-2 orbit exhibited by the system for $g^* \in (25.8, 30.5)$ [see Fig. 8(a)] undergoes a period-doubling bifurcation at $g^* = 30.5$. Then, the new period-4 orbit becomes tangent to the switching surface for $g^* \simeq 31.5$ [see Fig. 8(b)] and the system starts evolving along the chaotic attractor shown in Fig. 8(c). This chaotic attractor is then suddenly enlarged for $g^* > 32.0$, as shown in Fig. 8(d), when a further border-collision of one of its inner lobes takes place.

These results confirm that, as conjectured, many of the observed dynamical oddities exhibited by the PWL model of the Colpitts oscillator, such as the sudden jump to chaos, are the direct consequence of border-collision bifurcations.

B. Using Feigin's Method

The phenomena reported in the previous section can be analyzed by using the classification method due to Feigin described in Section IV-B. In order to clarify the application of this strategy to the model of the Colpitts we are studying, we will detail, without loss of generality, the case of the border-collision bifurcation occurring for $Q = 2.5$ and $g^* \simeq 16.578$ for decreasing values of g^*, as illustrated in Fig. 7.

As already mentioned, the first step consists of choosing an appropriate Poincaré section. This cannot be the switching surface $x_2 = 1$, hence we choose the hyperplane $x_3 = 0$ instead as our Poincaré surface. We now perturb the system parameter in a sufficiently small neighborhood of the border-collision bifurcation, i.e., $g^* \in (16.5, 16.6)$, and compute the eigenvalues L_1 and L_2 of the Jacobian matrices of the fixed points associated with the system orbit on each side of the border-collision. The following values were found:

g^*	L_1	L_2
16.5000	−0.0126	−0.7454
16.6000	0.0718	0.1311.

We can now compute the quantities required by Feigin's method. Namely, we have $\sigma_m^+ = 0$, $\sigma_m^- = 0$, $\sigma_p^+ = 0$, and $\sigma_p^- = 0$. Therefore, since $\sigma_m^- + \sigma_p^- = 0$ is even and $\sigma_m^+ + \sigma_p^+ = 0$ is even, we can conclude that at the border-collision, the grazing orbit will undergo a smooth transition into an orbit of a similar type having a section lying in the other region. This is precisely what is observed numerically and reported in Figs. 6 and 7.

The same theoretical framework can be applied to classify other border-collision bifurcations occurring in the PWL model of the Colpitts considered here.

C. Infinite Local Stretching

We now investigate the occurrence of infinite local stretching, described in Section IV and [10], in our PWL model of the Colpitts oscillator. In so doing, we consider the Poincaré map (also called *switching* or *impact* map in [10]) obtained by sampling the system states whenever the system trajectory crosses the switching surface $x_2 = 1$. This 2-D mapping Π takes the form:

$$\Pi \equiv (\pi_1, \pi_2): \left(x_{p1}^{(n)}, x_{p2}^{(n)}\right) \longrightarrow \left(x_{p1}^{(n+1)}, x_{p2}^{(n+1)}\right)$$

where $x_{p1} = x_1$, $x_{p2} = x_3$, and the indexes $(n, n+1)$ refer to two successive intersections of the system trajectory with the

[2]This also means that the Poincaré section $x_2 = 1$ is not a global one, i.e., it is not transversal to all the parts of the system solution.

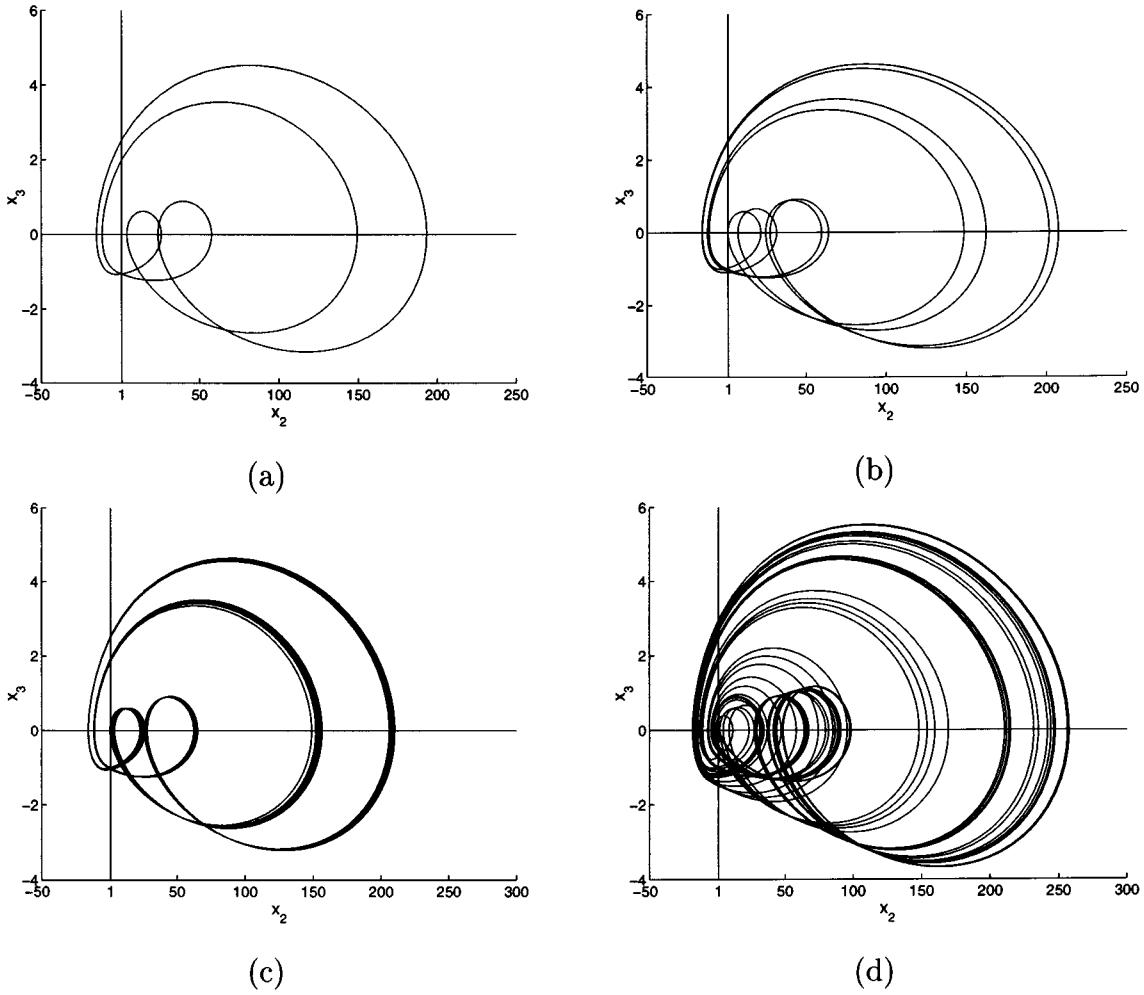

Fig. 8. Sudden jump to chaos and enlargement of the chaotic attractor for $Q = 2.5$: (a) Period-2 orbit at $g^* = 30.0$, undergoing period-doubling at $g^* \simeq 30.5$. (b) Period-4 orbit immediately before the border-collision bifurcation point at $g^* = 31.5$. (c) Chaotic attractor at $g^* = 31.75$, generated after the border-collision; notice that some of its inner lobes are getting closer to the switching plane. (d) Chaotic evolution at $g^* = 32.25$ after the enlargement (due to a border-collision) of the chaotic attractor depicted in (c).

Poincaré section $x_2 = 1$ (for instance with $\dot{x_2} > 0$). We emphasize that

$$\Pi = \Pi(x_{p1}, x_{p2}; Q, g^*)$$

and that the "flight time," τ_p, between two successive intersections with the switching surface is also a function of x_{p1} and x_{p2}; hence, $\tau_p^{(n)} = \tau_p^n(x_{p1}^{(n)}, x_{p2}^{(n)})$. The Jacobian of the Poincaré map is then defined as

$$J = \begin{pmatrix} J_{11} & J_{12} \\ J_{21} & J_{22} \end{pmatrix} = \begin{pmatrix} \dfrac{\partial x_{p1}^{(n+1)}}{\partial x_{p1}^{(n)}} & \dfrac{\partial x_{p1}^{(n+1)}}{\partial x_{p2}^{(n)}} \\ \dfrac{\partial x_{p2}^{(n+1)}}{\partial x_{p1}^{(n)}} & \dfrac{\partial x_{p2}^{(n+1)}}{\partial x_{p2}^{(n)}} \end{pmatrix}$$

where, by using implicit differentiation

$$J_{ij} = \frac{\partial x_{pi}^{(n+1)}}{\partial x_{pj}^{(n)}} = \frac{\partial \pi_i}{\partial x_{pj}} + \frac{\partial \pi_i}{\partial \tau_p}\frac{\partial \tau_p}{\partial x_{pj}}, \qquad i, j = 1, 2. \quad (6)$$

In order to derive the elements of the Jacobian J explicitly, we can now exploit the analytical solution of (3) in each linear region and use the switching constraint $x_2 = 1$. In particular, by denoting with $\Phi \equiv (\phi_1, \phi_2, \phi_3)$ the system solution and starting from the initial conditions (x_{10}, x_{20}, x_{30}) we have

$$\begin{aligned} x_1(\tau) &= \phi_1(x_{10}, x_{20}, x_{30}, \tau; Q, g^*) \\ x_2(\tau) &= \phi_2(x_{10}, x_{20}, x_{30}, \tau; Q, g^*) \\ x_3(\tau) &= \phi_3(x_{10}, x_{20}, x_{30}, \tau; Q, g^*). \end{aligned}$$

By imposing the switching condition at $x_2 = 1$ we get that

$$\phi_2(x_{10}, 1, x_{30}, \tau_p; Q, g^*) - 1 = 0$$

and by implicit differentiation, we can derive the terms

$$\frac{\partial \tau_p}{\partial x_{pj}} = -\left(\frac{\partial \phi_2}{\partial x_{pj}}\right)\left(\frac{\partial \phi_2}{\partial \tau_p}\right)^{-1}, \qquad j = 1, 2$$

that can be used to obtain the elements of the Jacobian (6).

Notice that the term $((\partial\phi_2)/(\partial\tau_p))$ is the derivative of the coordinate x_2 at the switching instant. Hence, at a border collision ($\dot{x}_2 = 0$), the term $((\partial\phi_2)/(\partial\tau_p))^{-1} \to \infty$. Consequently, at a border-collision bifurcation, one eigenvalue of the Jacobian tends to infinity (the other eigenvalue tending toward zero) and, as expected, infinite local stretching is introduced on the state space. This has been confirmed numerically for the Colpitts oscillator, as shown in Fig. 9.

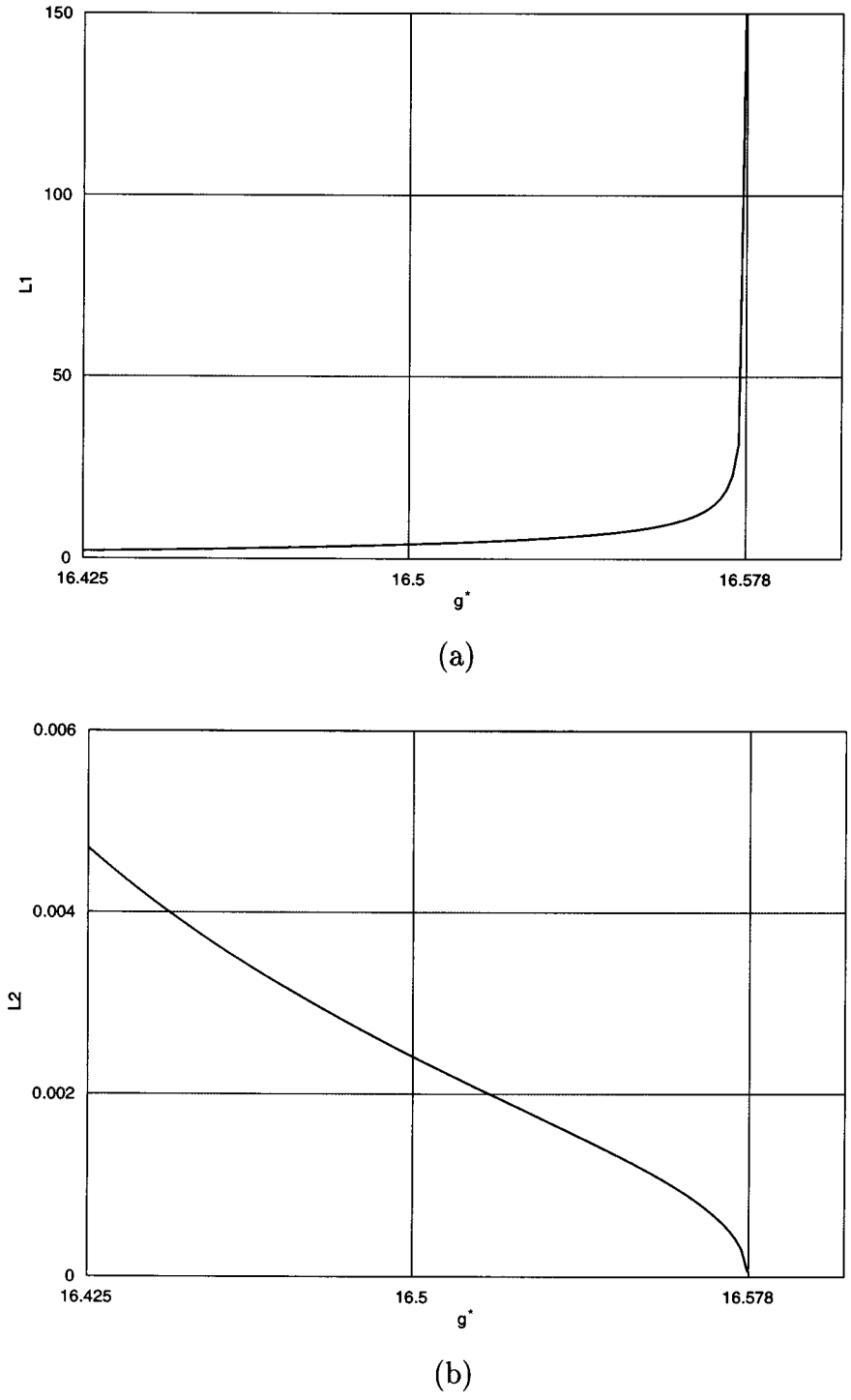

Fig. 9. Plots of eigenvalues, L_1, L_2, of the Poincaré map Π, defined with respect to $x_2 - 1$, versus g^*, for $Q = 2.5$: (a) L_1 versus g^*; note that $L_1 \to \infty$ when g^* approaches the value ($g^* - 16.578$) for which a border-collision bifurcation occurs. (b) L_2 versus g^*; at the border collision $L_1 \to 0$.

D. Other Nonsmooth Phenomena

In [11], it has been shown that other nonsmooth phenomena can play an important role in organizing the dynamics of a PWL system. For instance, it was shown that *sliding* orbits can be particularly relevant. These are periodic solutions that lie partly within the discontinuity set of the system of ODE's considered.

Here, we show that such solutions cannot occur in the case of our model of the Colpitts oscillator. In fact, these orbits would correspond to trajectories lying on the plane $x_2 = 1$. The following theorem shows that this is not possible for the Colpitts oscillator.

Theorem 1: The PWL model (3) for the Colpitts oscillator does not admit a sliding mode, i.e, a trajectory of (3) cannot evolve indefinitely along the surface of discontinuity $x_2 = 1$.

Proof: A sliding mode can occur for the model (3) only if the condition $\dot{x}_2 = 0$ is satisfied all along the sliding trajectory, i.e., for $x_2 = 1$. But $\dot{x}_2 = 0 \iff x_3 = 0$. It

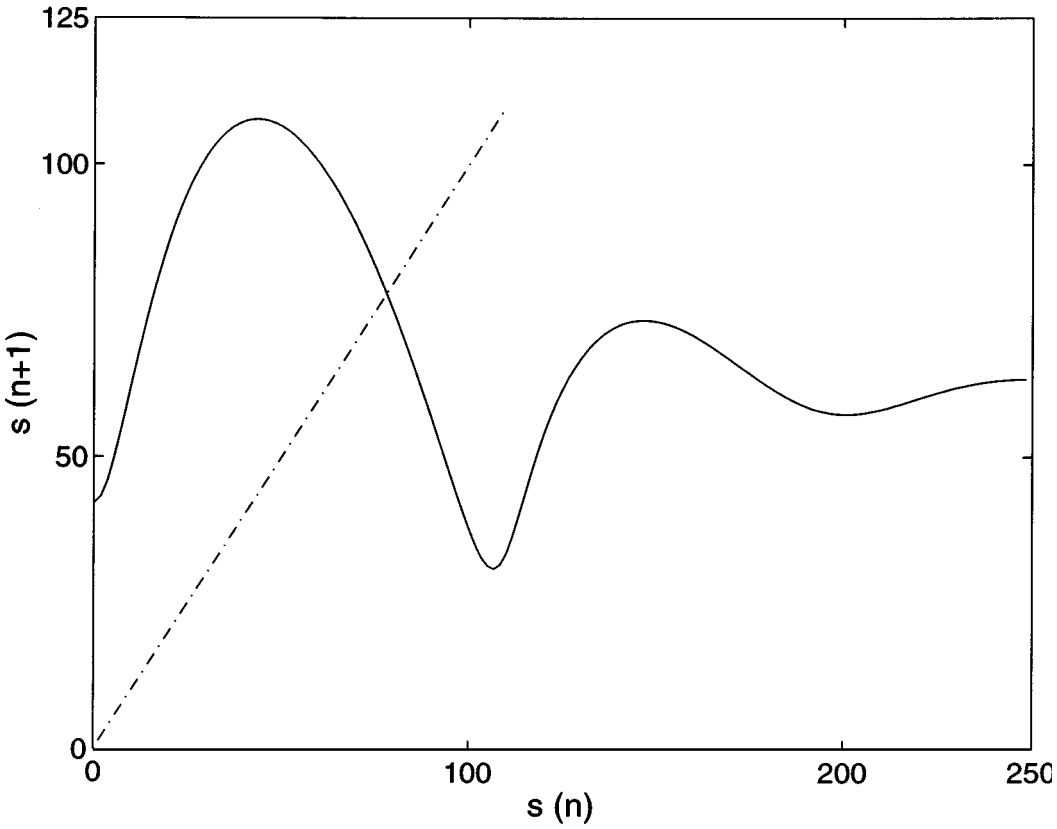

Fig. 10. Approximate 1-D map h: $s(n) \mapsto s(n+1)$ for $Q = 1.35$ and $g^* = 10$.

follows that sliding mode should necessarily occur on the line λ: $\{x_2 = 1, x_3 = 0\}$. This in turn requires that $\dot{x}_3 = 0$ to prevent a (potential) sliding trajectory from escaping from the line λ. Referring to the third equation of system (3) and by substituting: $x_2 = 1$ and $x_3 = 0$, it follows that, on the line λ, $\dot{x}_3 = 0 \iff x_1 = -1$. Now, let's suppose we set the system initial conditions as $x_{1o} = -1$, $x_{2o} = 1$, $x_{3o} = 0$. From the first equation of (3) we observe that $\dot{x}_1 > 0$. Hence, initially the sliding trajectory will evolve along the line λ in the direction of increasing x_1, but immediately it will start to deviate from $x_2 = 1$, because $\dot{x}_3 > 0$ and $\dot{x}_2 > 0$. We conclude then that no trajectory can lie on the plane $x_2 = 1$ and thus no sliding mode is possible for our PWL model of the Colpitts oscillator. ■

VI. Bifurcation Analysis Through a 1-D Map

A. An Approximate 1-D Map

In [15], an approximate 1-D discrete-time model was derived from the PWL model for the Colpitts oscillator. The derivation of this map can be briefly summarized as follows. First, a Poincaré section is fixed at $x_2 = 1$. The Poincaré intersections with $\dot{x}_2 > 0$ are then approximated by means of the line Λ, the intersection of the unstable eigenplane E^U in the forward active region with the Poincaré plane $x_2 = 1$ (see Fig. 5). Namely, the points of intersection are projected onto Λ along the direction (E^S) of the stable eigenvector in the forward active region. In so doing, we exploit the fact that trajectories in the forward active region are flattened (onto the unstable eigenplane) along that direction. A (unit speed) parameter s is then defined along the line Λ. In this way, it is possible to construct a 1-D, single-valued, noninvertible map h by plotting $s(n+1)$ versus $s(n)$, where the index n refers to the order in which the trajectory of the dynamical system associated with the Colpitts oscillator intersects the Poincaré plane $x_2 = 1$. An instance of this map for $Q = 1.35$ and $g^* = 10$ is given in Fig. 10.

The 1-D map derived above gives a good approximation of the dynamics of the PWL model of the Colpitts oscillator under investigation. This can be seen clearly from Fig. 11 where a comparison of the two-parameter bifurcation diagrams obtained by considering the PWL model for the Colpitts oscillator and the approximate 1-D map h, respectively, is reported.

B. Discontinuities of the 1-D Map

We now discuss the occurrence of discontinuities in the graph of the 1-D map h described in the previous section and relate these to the corresponding tangencies with the switching surface (border-collisions) of the trajectories of the PWL model for the Colpitts oscillator.

Let's consider the graph of h for $Q = 2$ and $g^* = 10$, shown in Fig. 12. We note that the approximate 1-D map h presents a discontinuity when the coordinate along the line Λ has a value $s = s_d = 80.668$. We now follow the evolution in state space of a trajectory starting from the initial point P_d in state space, corresponding to the coordinate $s = s_d$, along Λ. We remark that according to the mapping procedure described in Section VI-A,

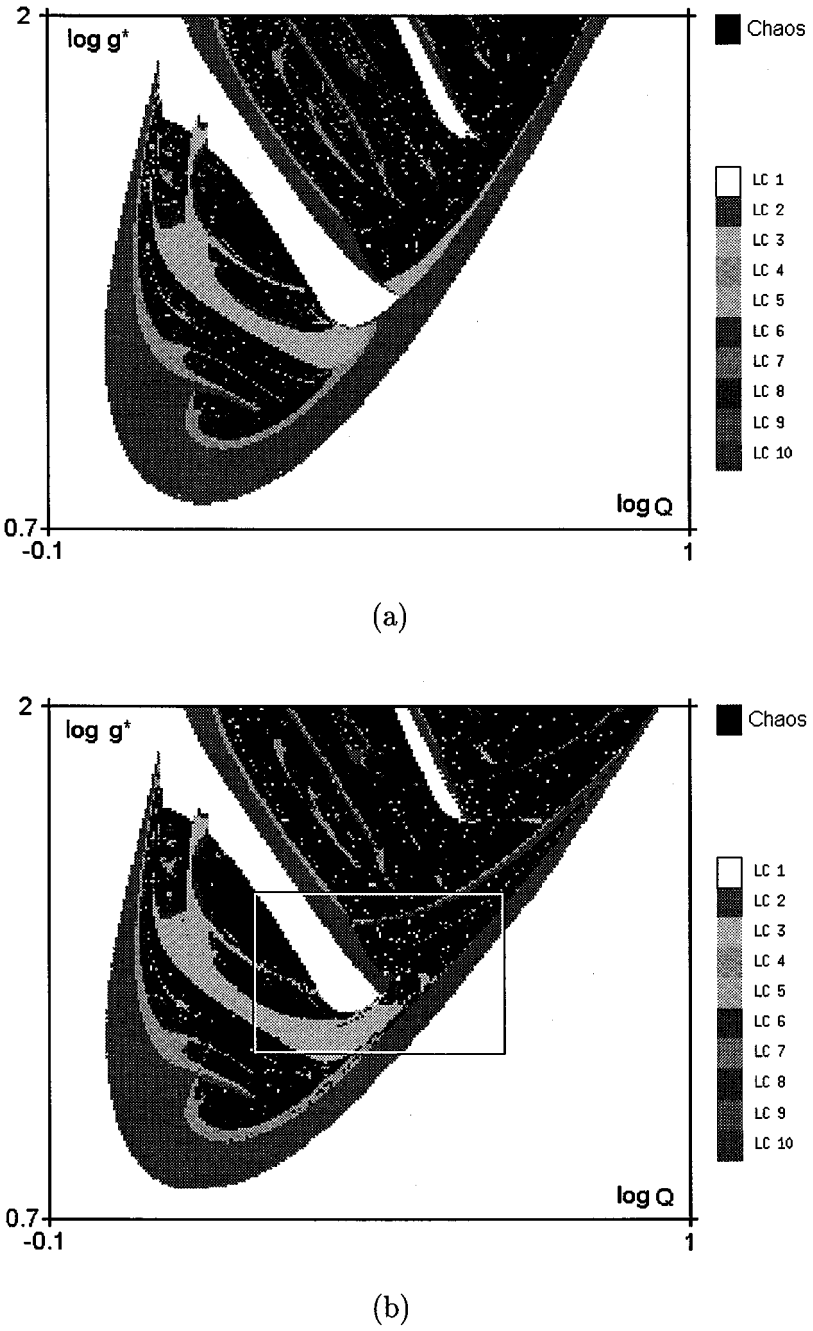

Fig. 11. Two-parameter bifurcation diagram (by simulation). (a) Piecewise-linear model. (b) Approximate 1-D map. The 1-D map of the Colpitts oscillator preserves the qualitative dynamical behavior of the PWL model. The bifurcations occurring in the boxed region are illustrated in Fig. 15.

there is a unique point P_d on the line Λ in state space, corresponding to s_d. As depicted in Fig. 13(a) and (b), it is clear that the system trajectory starting from $P(n) = P_d$ (corresponding to $s = s_d$) is a trajectory that just grazes the switching plane $x_2 = 1$ tangentially. It follows that the discontinuity observed in the 1-D map for $s = s_d$ can be seen as the result of a border-collision of the trajectory originating at point P_d. However, in general this does *not* correspond to a border-collision bifurcation of the original PWL system, but it is related to the way the 1-D map is constructed. We emphasize that a discontinuity in the 1-D map indicates the occurrence of a border-collision in the PWL system *only* when the discontinuity occurs at a fixed point (of some order n) of the 1-D map itself.[3]

In conclusion, the jump in the value of $s(n+1)$ exhibited by the 1-D map is caused by the phase shift characterizing trajectories starting from points close to the coordinate s_d, but on opposite sides with respect to it. Again, this reflects the fact that the Poincaré section chosen to construct the 1-D map is not global. Nevertheless, the resulting 1-D map is useful for analyzing the dynamics of the Colpitts oscillator. Namely, by ex-

[3]This is a direct consequence of the fact that orbits of the PWL model correspond to (stable) fixed points, of some order n, for the approximate 1-D map.

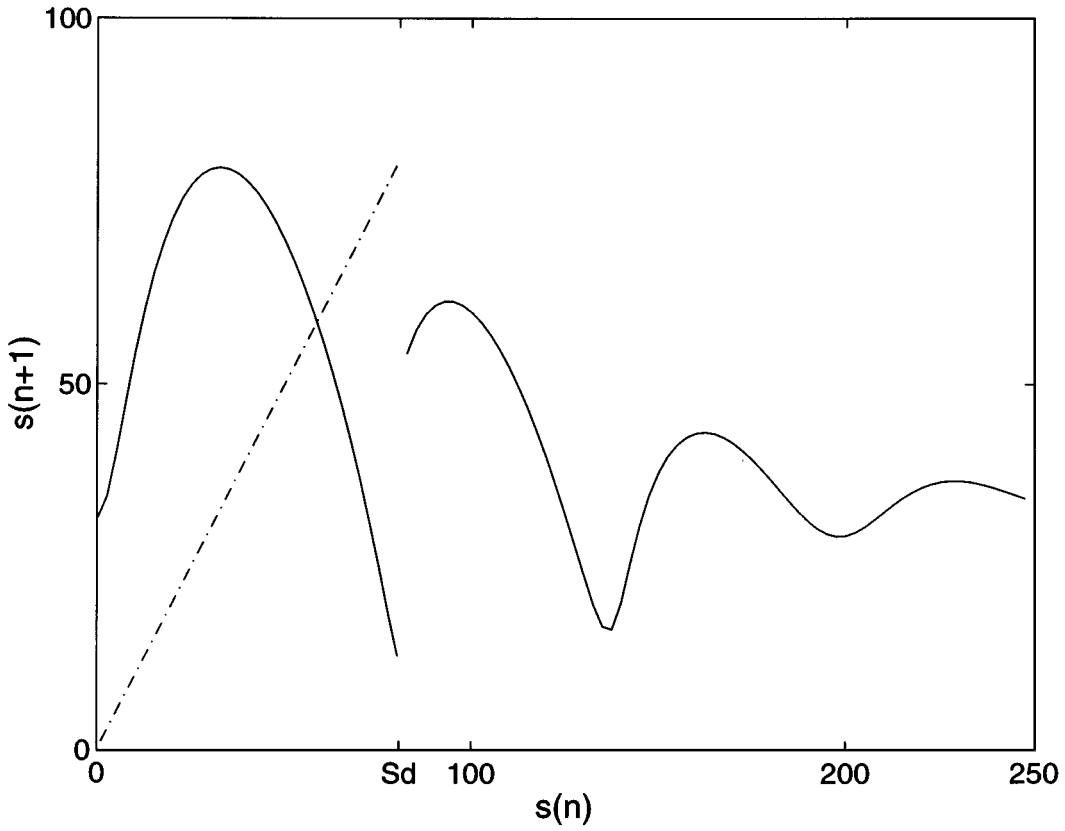

Fig. 12. 1-D map h with discontinuity for $Q = 2$ and $g^* = 10$.

ploiting the sensitivity of the 1-D map to border-collision bifurcations, we will show in Section VI-D how it can be exploited for performing an analysis of the nonsmooth bifurcations of the PWL model (3).

C. Analysis of Singularities

We now focus our attention on analyzing the kind of discontinuities of the 1-D map described in Section VI-B. In particular, we will analyze the situation when a border-collision bifurcation occurs in the PWL system. For instance, this is the case that will be discussed in Section VI-D [see Fig. 17(d), for $Q = 2.5$ and $g^* = 16.578$], for which a discontinuity occurs at a fixed point of the 1-D map h.

For this study, we will consider for convenience the return map, h_3: $x_3(n) \mapsto x_3(n+1)$, obtained by plotting the iterates of the coordinate $x_3(n)$ of the point $P(n)$, in state space, corresponding to the point $s(n)$ on the line Λ.

Fig. 14(a) shows the graph of h_3 for $Q = 2.5$ and $g^* = 16.578$. We note the presence of a discontinuity when $x_3(n+1) = 0$. This is consistent with the hypothesis that the discontinuity is due to a border-collision bifurcation. In fact, when such a bifurcation occurs, the state space trajectory becomes tangent to the switching surface, i.e., $x_2 = 1$ and $\dot{x}_2 = x_3 = 0$; hence the discontinuity observed for $x_3(n+1) = 0$. Further investigations reveal that locally, near the bifurcation point, the map h_3 exhibits a square-root-like singularity, as illustrated in Fig. 14(b) and (c). In particular, in Fig. 14(b), we observe that relatively far from the point of discontinuity $x_{3d} = 2.5029853$, the map decays linearly with x_3, that is following a scaling law of the type: $x_3(n+1) \sim (x_{3d} - x_3(n))$. As we get closer to x_{3d}, though, the scaling follows more and more closely a square-root-like behavior, i.e., $x_3(n+1) \sim (x_{3d} - x_3(n))^{1/2}$.

This yields the interesting conclusion that even border-collision bifurcations (occurring in systems which are *continuous but nonsmooth* across the border) can be characterized under certain conditions by normal forms containing a square root singularity as in the case of grazing bifurcations (occurring in system whose flow is *discontinuous* across the border).

We conjecture here that the appearance of the square-root singularity is related to the gradient of the piecewise-linear term acting on the system on each side of the border. Namely, by looking at the PWL model (3) of the Colpitts, we see that the PWL term $n(x_2)$ is equal to $-x_2$ in one region while it is constant on the other region. Hence, when the system flow crosses the border, the reciprocal of the gradient of the piecewise linearity $n(x_2)$ goes from -1 to $-\infty$. We conjecture that it is this nonfinite value of the reciprocal gradient that causes the square-root-like singularity exhibited by the 1-D map at the border-collision bifurcation. The detailed analysis of this situation is currently under investigation and will be published elsewhere.

D. Bifurcation Analysis

We will now show how the 1-D map described above can be used to carry out a bifurcation analysis of the model under investigation. We will focus our attention on the boxed region of

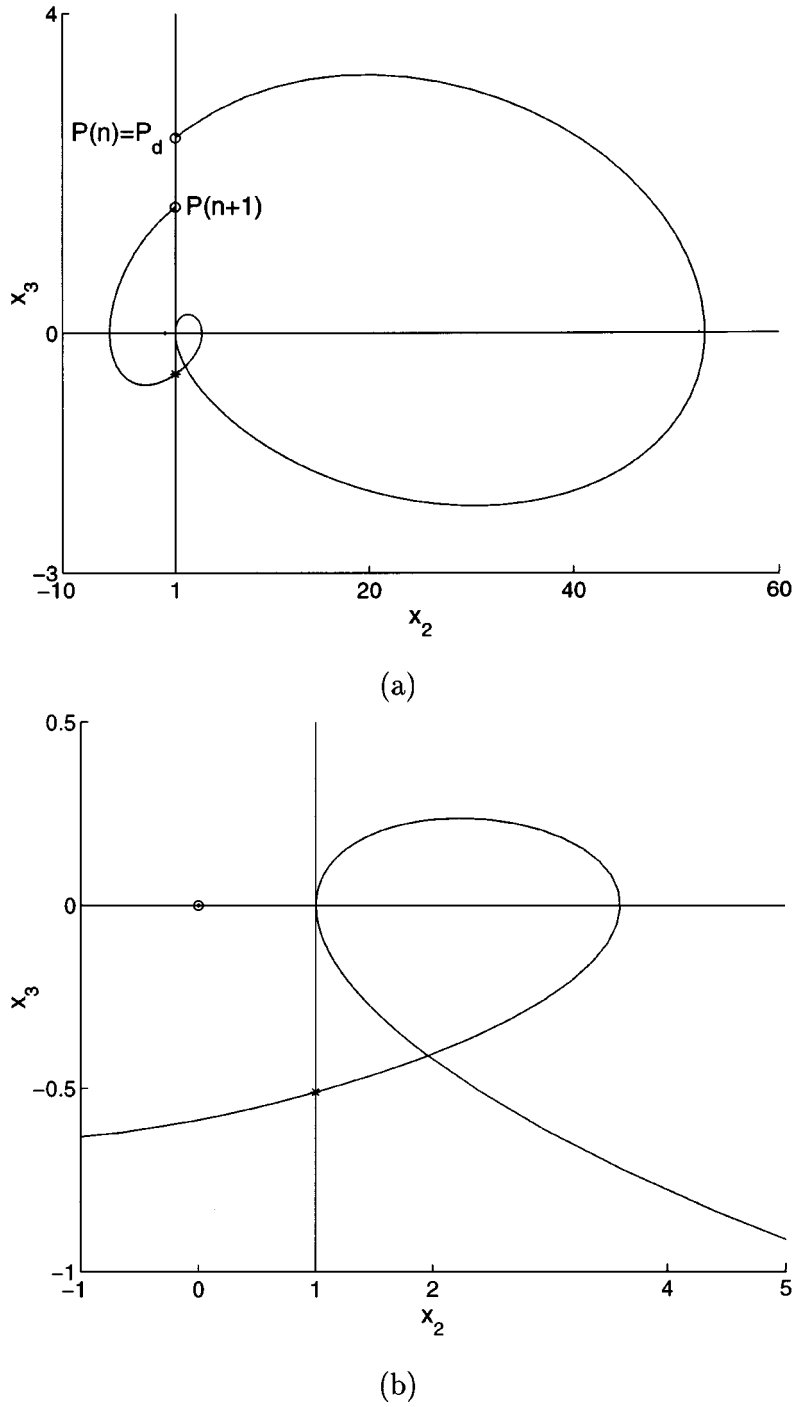

Fig. 13. Two-dimensional state-space projection at the discontinuity for $Q = 2$ and $g^* = 10$: (a) Trajectory for $s = s_d$; the starting point P_d is the point in state space corresponding to the coordinate s_d along the line Λ. (b) Detail of the grazing trajectory.

the two-parameter bifurcation diagram in Fig. 11(b), and shown in detail in Fig. 15. Note that the bifurcation results presented in this section have been obtained by brute force simulation of the 1-D map h throughout the parameter region in Fig. 15.

Furthermore, it should be noted that the analysis reported here, which is based on the two-parameter bifurcation diagram of the approximate 1-D map holds, without substantial modifications, also for the PWL model of the Colpitts (from which the map has been derived). Hence, in the sequel we will refer generically to bifurcations of the 1-D map and to the corresponding bifurcations of the PWL system. We remark that a stable fixed point for the 1-D map corresponds to a (stable) periodic orbit for the PWL model. The notation that we will adopt henceforth for the fixed points s_{fp} will be to indicate their stability properties, or the kind of bifurcation that the fixed point undergoes, and the corresponding slope $h'(s_{fp})$ of the 1-D map at the fixed point. We recall that a fixed point of h is stable (S) if $|h'(s_{fp})| < 1$ and unstable (U) if $|h'(s_{fp})| > 1$.

In describing the smooth and nonsmooth bifurcations that a system orbit undergoes when the parameters Q and g^* are

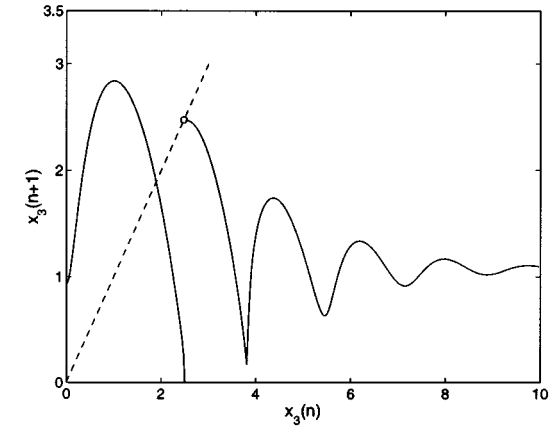

(a)

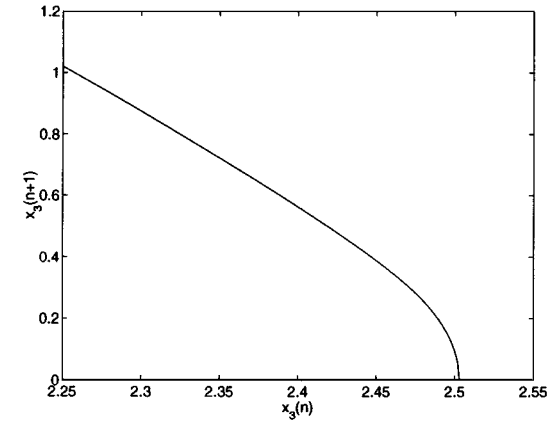

(b)

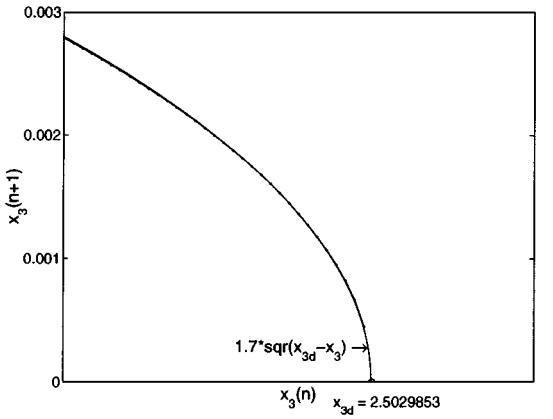

(c)

Fig. 14. Singularity in the return map h_3: $x_3(n) \mapsto x_3(n+1)$. (a) Graph of h_3 for $Q = 2.5$ and $g^* = 16.578$. (b) Zoom close to the singularity point. (c) Detail of the square-root-like singularity.

varied, we will refer to the generic period-1 orbit existing in the central white area of the region represented in Fig. 15. A typical instance of this type of orbit is the one shown in Fig. 16, corresponding to point $\boldsymbol{O}$ in Fig. 15. In order to analyze the bifurcations associated with this one-periodic orbit, we will imagine moving the parameters along the path **a-b-c-d-e-f** indicated in Fig. 15. The corresponding graphs of the 1-D map h are reported in Fig. 17.

Starting from the point **a** that corresponds to a chaotic evolution we observe the "birth" of a periodic orbit when the value of g^* is increased up to the point **b**. This corresponds to the *tangent* (or *fold*) bifurcation occurring along the curve indicated by T in Fig. 15. This smooth bifurcation is characterized by the creation of a new stable (plus an unstable) periodic orbit, as shown in Fig. 18(a) and (b), where the state-space trajectories corresponding to the points **a** and **b**, respectively, are reported. The same phenomenon can be analyzed in terms of the 1-D map, as reported in Fig. 17(a) and (b), where we show that the 1-D map undergoes a tangent bifurcation when the parameters are moved from point **a** to **b**. The creation of a new stable fixed point corresponds to the period-1 orbit observed in state space. Also, note that in the case of chaotic evolution the corresponding 1-D map reported in Fig. 17(a) admits only an unstable fixed point.

We now vary the parameters Q and g^* in order to move from point **b** to point **c** along the path depicted in Fig. 15. This point is located at the intersection of the curve T of tangent bifurcation with the curve $BC+$. The latter curve represents the locus in parameter space of border-collision bifurcations associated with the creation of a stable period-1 solution (corresponding to a stable fixed point of the 1-D map). Conversely, $BC-$ indicates the locus of border-collision bifurcations associated with an unstable fixed point of the 1-D map. The graph of h at point **c** is reported in Fig. 17(c). As we can see at this point, the 1-D map presents a discontinuity coinciding with a fixed point. This confirms that a border-collision bifurcation is taking place. Moreover, notice that $h'(s_{fp}) = +1$ at the discontinuity, which is reminiscent of a tangent bifurcation.

We then move to point **d** in Fig. 15. This point is lying on the curve $BC+$ and is a typical example of a border-collision bifurcation generating a stable periodic orbit. The corresponding graph of h is reported in Fig. 17(d) from which the creation of a stable fixed point ($|h'(s_{fp})| < 1$) is clearly visible.

A detailed analysis of the border-collisions occurring at point **d** (for $Q = 2.5$ and $g^* \simeq 16.578$) has already been presented in Section V.

By increasing the value of g^*, for fixed $Q = 2.5$ ($\log Q \simeq 0.4$), we now move on to the period-1 orbit at point $\boldsymbol{O}$, shown in Fig. 16 and we discuss the *period-doubling* or *flip* bifurcation that this orbit undergoes at point **e**. The graph of h at point **e** is reported in Fig. 17(e), where a fixed point with $h'(s_{fp}) = -1$ is visible. This clearly indicates the occurrence of a flip bifurcation. Moreover, this smooth bifurcation is illustrated in Fig. 18(c) and (d), where the orbits of the PWL systems for values of g^* slightly smaller and larger than the one corresponding to **e** are shown. From the latter, the period-doubling of the orbit is evident.

The curve denoted by F in Fig. 15 corresponds to the locus in parameter space where the generic period-1 orbit (of the same kind as the one at point $\boldsymbol{O}$) existing in the region under consideration undergoes a flip bifurcation. In particular, at point

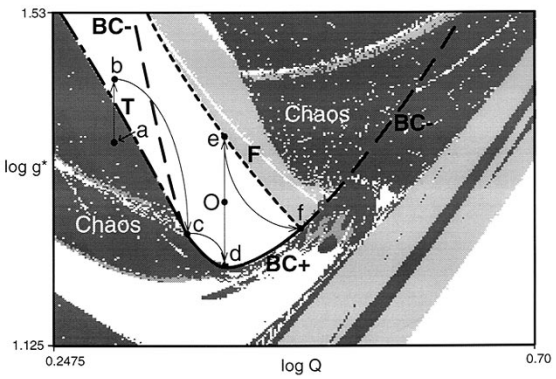

Fig. 15. Bifurcation diagram of the 1-D map for the boxed region of Fig. 11(b). The bifurcation curves have been obtained by extensive simulation of the 1-D map h. The curves T and F correspond to tangent and flip (smooth) bifurcations of the period-1 orbit at point $\boldsymbol{O}$, respectively. The (nonsmooth) bifurcation curve BC denotes the locus in the parameter space where a border-collision takes place, either of a stable $(+)$ or of an unstable $(-)$ orbit.

f the curve F intersects the locus $BC+$ corresponding to a border-collision of the (stable) period-1 orbit. The graph of h at point **f** is reported in Fig. 17(f) where the 1-D map exhibits a discontinuity at a fixed point characterized by a slope $h'(s_{fp}) = -1$; this is reminiscent of a flip bifurcation.

E. Smooth versus Nonsmooth Bifurcations

To conclude our analysis we now discuss the transition from smooth to nonsmooth bifurcations, referring to Feigin's theory presented in Section IV-B. In order to apply Feigin's criterion to analyze the bifurcations of the 1-D map we remark that in this case the eigenvalues of the mapping describing the local dynamics in the neighborhood of a fixed point coincide with the slope of the 1-D map at the fixed point itself.

In particular, we focus our attention on the points **c** and **f** in Fig. 15. As already pointed out, at these points the smooth bifurcation curves T and F intersect the border-collision bifurcation curve $BC+$. The behavior at point **c** is qualitatively similar to the one observed when the system undergoes a smooth tangent bifurcation. In fact, from Fig. 17(c) we can see that $h'(s_{fp}) = +1$. Hence, according to Feigin's theory the sudden appearance (or disappearance) of a periodic orbit is expected. This can be verified by looking at the map slopes—eigenvalues—at the stable fixed points in Fig. 17(b) and (c), from which it follows that $\sigma_m^+ + \sigma_p^+$ is an odd number.[4] Therefore, point **c** can be seen as the point at which a tangent bifurcation, characterized by $h'(s_{fp}) = 1$, and a border-collision bifurcation are qualitatively similar. Similarly, we observe that at point **f** in Fig. 15 the 1-D map h, depicted in Fig. 17(f), undergoes a border-collision bifurcation that is qualitative similar to a flip bifurcation, for which $h'(s_{fp}) = -1$. Again, this is in agreement with what is predicted by Feigin's theory since, by looking at the slopes of the 1-D map at the fixed points, we can deduce that at the

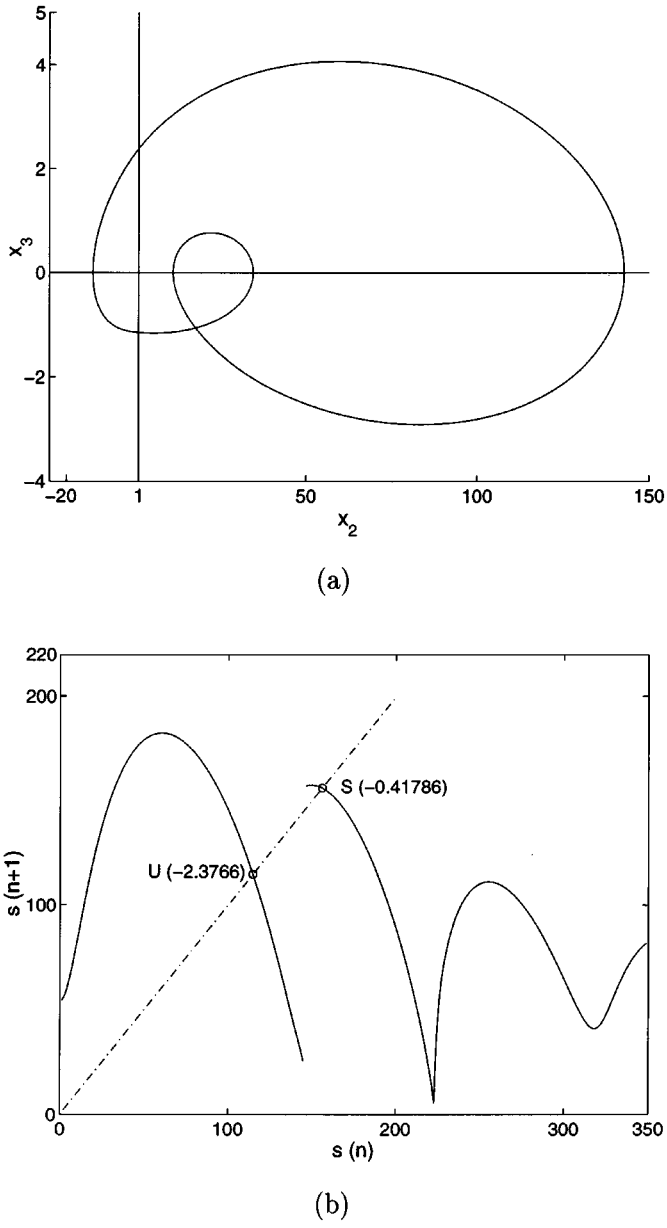

Fig. 16. Period-1 orbit at point $\boldsymbol{O}$ ($\log\ Q = 0.398$ and $\log\ g^* = 1.3$). (a) Two-dimensional state space view. (b) Corresponding graph of the 1-D map h. Note that the periodic orbit (a) corresponds to the stable fixed point S.

border-collision point **f**, $\sigma_m^- + \sigma_p^-$ is an odd quantity.[5] Hence, point **f** can be considered as the point at which a flip bifurcation, characterized by $h'(s_{fp}) = -1$, and a border-collision bifurcation become qualitatively similar.

This analysis confirms that border-collision bifurcations are an important class of bifurcations in organizing the dynamics of the PWL model of the Colpitts oscillator which we have considered. Also, the 1-D map has been shown to be a particularly effective tool in carrying out a bifurcation analysis of the system.

Finally, our numerical observations suggest that border-collision bifurcations are in some sense the result of the degeneration (due to the nonsmoothness of the system) of conventional tangent and flip bifurcations, as conjectured in [27].

[4]Referring to Section IV-B, from Fig. 17(b), it follows $\sigma_m^+ = 0$ and, from Fig. 17(c), it follows $\sigma_p^+ = 1$; thus $\sigma_m^+ + \sigma_p^+ = 1$.

[5]In fact, from Fig. 17(b) it follows $\sigma_m^- = 0$ while, from Fig. 17(e), it follows $\sigma_p^- = 1$; thus $\sigma_m^- + \sigma_p^- = 1$.

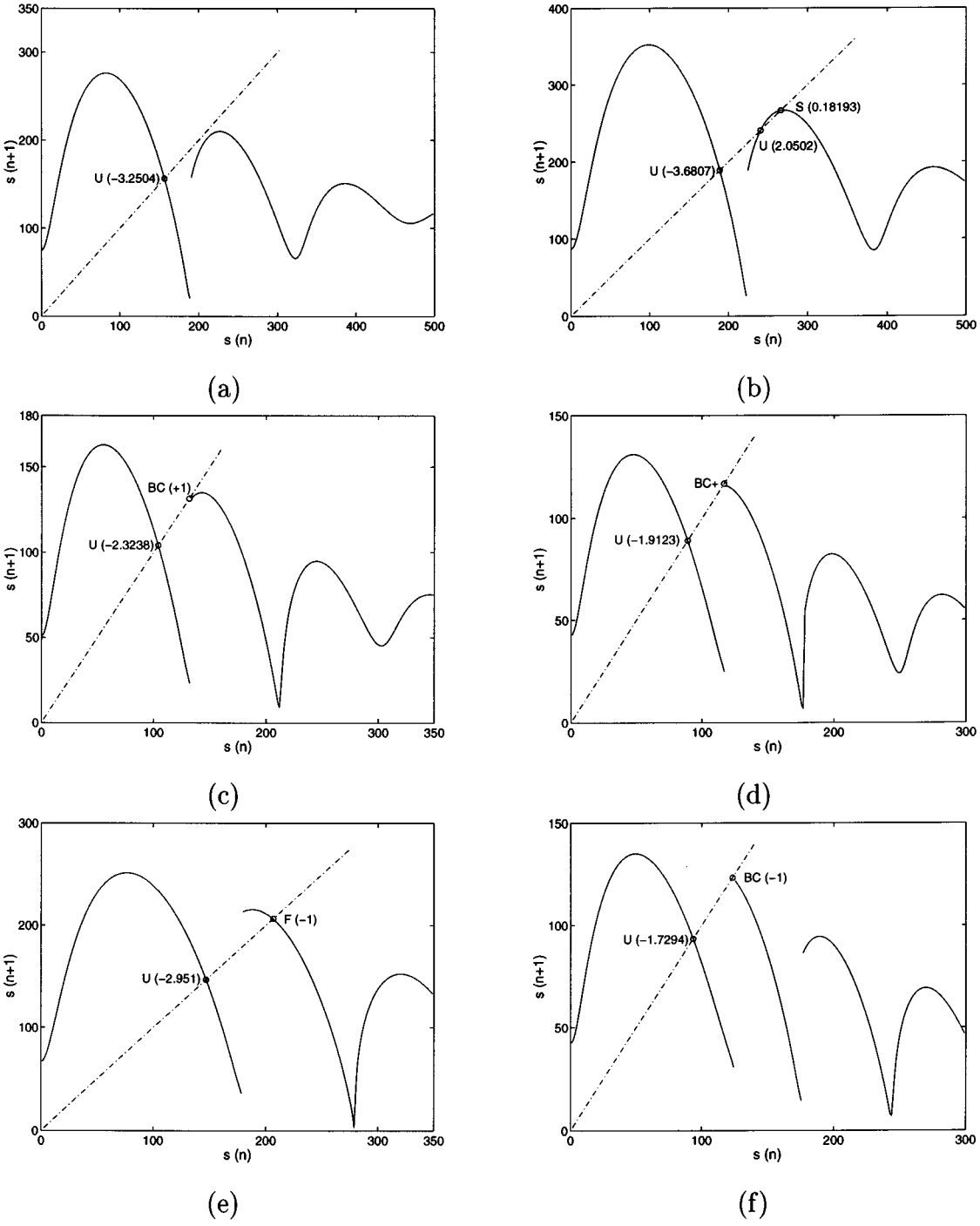

Fig. 17. Bifurcation analysis through the 1-D map, illustrating the (smooth and nonsmooth) bifurcations occurring along the path **a-b-c-d-e-f** in Fig. 15. (a) 1-D map at point **a** ($\log\ Q = 0.302, \log\ g^* = 1.373$) before the tangent bifurcation occurring on the curve T. (b) 1-D map at point **b** ($\log\ Q = 0.302, \log\ g^* = 1.447$) just after the tangent bifurcation. (c) 1-D map at point **c** ($\log\ Q = 0.368, \log\ g^* = 1.248$) corresponding to the transition from tangent to border-collision bifurcation. (d) 1-D map at point **d** ($\log\ Q = 0.398, \log\ g^* = 1.21$) on the curve $BC+$. (e) 1-D map at point **e** ($\log\ Q = 0.398, \log\ g^* = 1.3968$) at the flip bifurcation, on the curve F. (f) 1-D map at point **f** ($\log\ Q = 0.472, \log\ g^* = 1.251$) corresponding to the transition from flip to border-collision bifurcation.

VII. Conclusion

In this paper the occurrence of border-collision bifurcations in a PWL model of the Colpitts oscillator has been investigated. Conditions for border collisions in the Colpitts have been derived and a method to classify their occurrence has been presented and applied to the model under investigation.

Numerical evidence for the occurrence of several nonsmooth phenomena has been reported for different values of the system parameters and motivated as a direct consequence of this class of nonsmooth bifurcations. Moreover, a local analysis of the border collision has revealed that, also for the Colpitts oscillator, border collisions correspond to the occurrence of a singularity in the Jacobian of the system.

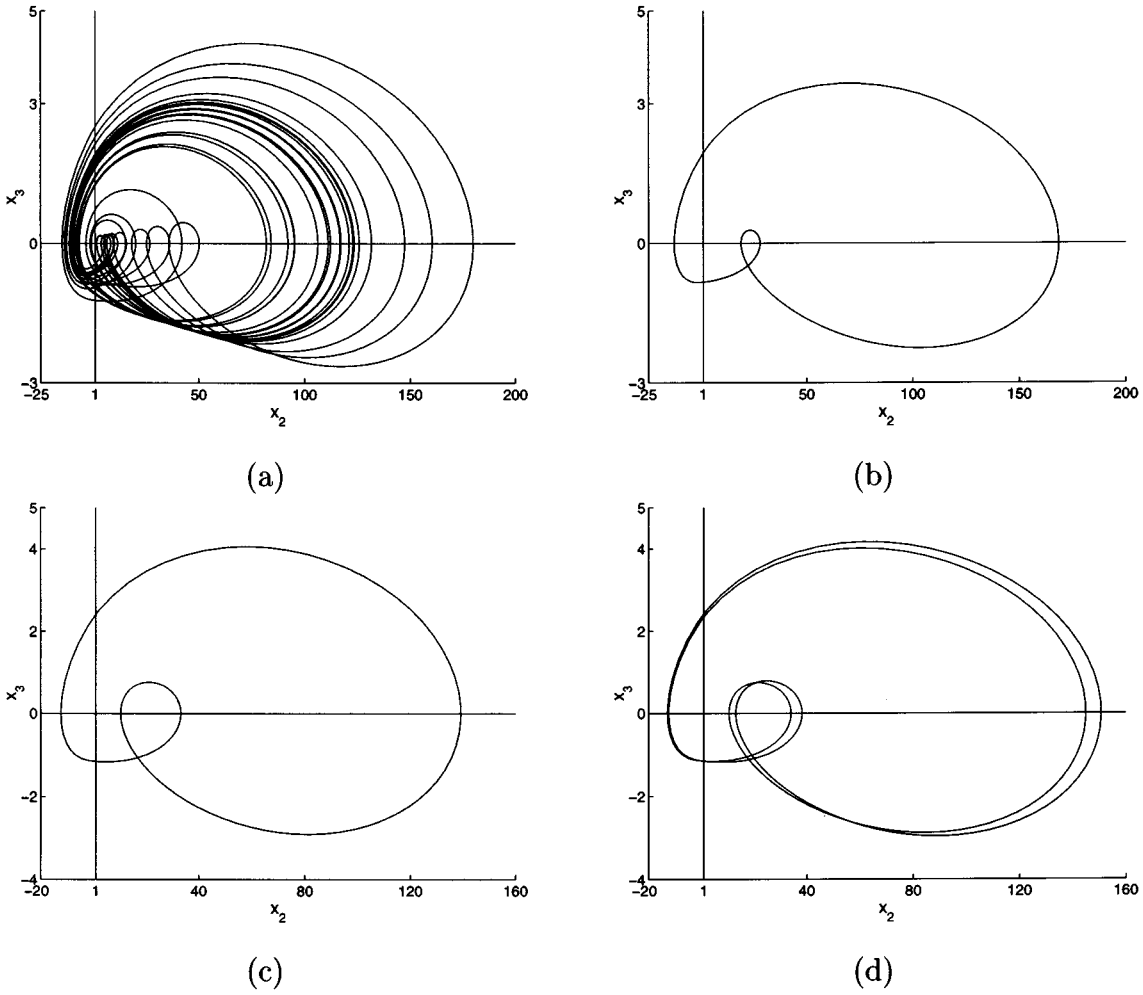

Fig. 18. Illustration of the smooth bifurcations of the PWL system occurring along the curves T and F. (a) Chaotic attractor, before the tangent bifurcation, at point **a** ($\log\ Q = 0.302, \log\ g^* = 1.373$). (b) Period-1 orbit born after the tangent bifurcation, at point **b** ($\log\ Q = 0.302, \log\ g^* = 1.447$). (c) Period-1 orbit before the flip bifurcation, below point **e** ($\log\ Q = 0.398, \log\ g^* = 1.389$). (d) Period-2 orbit after the flip bifurcation, above point **e** ($\log\ Q = 0.398, \log\ g^* = 1.41$).

Furthermore, we have shown that the occurrence of border-collision bifurcations can be detected by an approximate 1-D map of the Colpitts oscillator. In particular, this map exhibits square-root-like singularities reminiscent of those which are observed for grazing bifurcations of discontinuous systems.

Finally, the 1-D map has proven to be particularly useful for investigating the bifurcation phenomena, especially for pointing out the relationship between smooth and nonsmooth bifurcations in the system.

REFERENCES

[1] P. Pejovic and D. Maksimovic, "An algorithm for solving piecewise-linear networks that include elements with discontinuous characteristics," *IEEE Trans. Circ. Syst.—I*, vol. 43, pp. 453–460, June 1996.

[2] S. Pastore and A. Premoli, "Capturing all admissible linear regions for fast simulations of piecewise-linear dynamic circuits," in *Proc. ISCAS'96*, Atlanta, GA, May 12–15, 1996, pp. 253–256.

[3] L. O. Chua and A. Deng, "Canonical piecewise linear modeling," *IEEE Trans. Circ. Syst.—I*, vol. 33, pp. 511–525, 1986.

[4] H. Kawakami and R. Lozi, *Structure and Bifurcations of Dynamical Systems*. Singapore: World Scientific, 1992.

[5] M. Ohnishi and N. Inaba, "A singular bifurcation into instant chaos in a piecewise-linear circuit," *IEEE Trans. Circ. Syst.—I*, vol. 41, pp. 433–442, June 1994.

[6] T. Saito and S. Nakagawa, "Chaos from a hysteresis and switched circuit," *Phil. Trans. R. Soc. London A*, vol. 353, pp. 47–57, Nov. 1995.

[7] E. Freire, E. Ponce, F. Rodrigo, and F. Torres, "Bifurcations sets of continuous piecewise linear systems with two zones," *Int. J. Bifurc. Chaos*, vol. 8, pp. 2073–2098, Nov. 1998.

[8] S. Banerjee and C. Grebogi, "Border collision bifurcations in two-dimensional piecewise smooth maps," *Phys. Rev. E*, vol. 59, no. 4, pp. 4052–4061, 1999.

[9] A. Champneys, M. di Bernardo, L. Glielmo, F. Garofalo, and F. Vasca, "Nonlinear phenomena in DC/DC converters," in *Proc. NDES'96*, Seville, Spain, June 1996, pp. 51–56.

[10] M. di Bernardo, L. Glielmo, F. Garofalo, and F. Vasca, "Switchings, bifurcations and chaos in DC/DC converters," *IEEE Trans. Circ. Syst.—I*, vol. 45, pp. 133–141, Feb. 1998.

[11] M. di Bernardo, C. J. Budd, and A. R. Champneys, "Grazing, skipping and sliding: analysis of the nonsmooth dynamics of the DC/DC buck converter," *Nonlinearity*, no. 11, pp. 859–890, 1998.

[12] G. Yuan, S. Banerjee, E. Ott, and J. A. Yorke, "Border-collision bifurcations in the buck converter," *IEEE Trans. Circ. Syst.—I*, vol. 45, pp. 707–716, July 1998.

[13] M. P. Kennedy, "Chaos in the Colpitts oscillator," *IEEE Trans. Circ. Syst.—I*, vol. 41, pp. 771–774, Nov. 1994.

[14] G. M. Maggio, C. Kennedy, and M. P. Kennedy, "Experimental manifestations of chaos in the Colpitts oscillator," in *Proc. ISSC'97*, Derry, Ireland, June 26–27, 1997, pp. 235–242.

[15] F. O'Cairbre, G. M. Maggio, and M. P. Kennedy, "Devaney chaos in an approximate one-dimensional model of the Colpitts oscillator," *Int. J. Bifurc. Chaos*, vol. 7, pp. 2561–2568, Nov. 1997.

[16] G. M. Maggio, M. di Bernardo, and M. P. Kennedy, "Evidence of nonsmooth bifurcations in a piecewise-linear model of the Colpitts oscillator," in *Proc. NDES'98*, Budapest, Hungary, July 16–18, 1998, pp. 317–320.
[17] G. M. Maggio, O. De Feo, and M. P. Kennedy, "Nonlinear analysis of the Colpitts oscillator and applications to design," *IEEE Trans. Circ. Syst.—I*, vol. 46, pp. 1118–1130, Sept. 1999.
[18] H. E. Nusse, E. Ott, and J. A. Yorke, "Border-collision bifurcations—An explanation for observed bifurcation phenomena," *Phys. Rev. Lett. E*, no. 49, pp. 1073–1076, 1994.
[19] M. I. Feigin, "The increasingly complex structure of the bifurcation tree of a piece-wise smooth system," *J. Appl. Math. Mech.*, no. 59, pp. 853–863, 1995.
[20] M. di Bernardo, M. I. Feigin, S. J. Hogan, and M. A. Homer, "Local analysis of C-bifurcations in n-dimensional piecewise smooth dynamical systems," *Chaos Solitons Fractals*, vol. 10, no. 11, pp. 1881–1908, 1999.
[21] J. Millman and A. Grabel, *Microelectronics*, 2nd ed, ser. Electrical Engineering, Electronics and Electronic Circuits. Singapore: McGraw-Hill, 1988.
[22] S. Fraser and R. Kapral, "Analysis of flow hysteresis by a one-dimensional map," *Phys. Rev. A*, vol. 25, no. 6, pp. 3223–3233, 1982.
[23] H. E. Nusse and J. A. Yorke, "Border-collision bifurcations including "period-two to period-three" for piecewise smooth systems," *Physica D*, no. 57, pp. 39–57, 1992.
[24] ——, "Border collision bifurcations for piecewise smooth one-dimensional maps," *Int. J. Bifurc. Chaos*, no. 5, pp. 189–207, 1995.
[25] A. B. Nordmark, "Non-periodic motion caused by grazing incidence in an impact oscillator," *J. Sound Vibration*, vol. 145, no. 2, pp. 279–297, 1991.
[26] C. J. Budd and A. G. Lee, "Double impact orbits of a single-degree-of-freedom impact oscillator subject to periodic forcing of odd frequency," *Proc. R. Soc. A*, no. 452, pp. 2719–2750, 1996.
[27] S. Foale and S. R. Bishop, "Bifurcations in impact oscillators," *Nonlinear Dynam.*, no. 6, pp. 285–299, 1994.

Gian Mario Maggio (S'95–M'99) received a five-year honors degree in electronic engineering from the Politecnico di Torino, Italy, in March 1995 and carried out his graduation project at Trinity College, Dublin, Ireland. He was the recipient of a Marie Curie fellowship, and in February 1999, he obtained the Ph.D. degree in electronic engineering from University College Dublin, Ireland.

During 1995 he worked as an electronic designer in the Philips R&D Labs in Milan, Italy. Also, he collaborated on a research project with the Politecnico di Torino. He has visited the Swiss Federal Institute of Technology, Lausanne, the University of Bristol, U.K., the University of California, Berkeley, and the U.S. Army Research Office, Hunstville, AL. Since March 1999, he has been with the Institute for Nonlinear Science (INLS), at the University of California, San Diego. Recently, he has joined ST Microelectronics-San Diego as a research engineer in the wireless communication field. His research interests are in the area of analog circuit design, oscillators, nonlinear dynamics of electronic circuits, and chaotic communication systems.

Dr. Maggio received the Best Paper Award at the European Conference on Circuit Theory and Design 1999.

Mario di Bernardo (S'95–A'98) was born in Naples, Italy, on May 11, 1970. He received a five-year honors degree in electronic engineering from the University of Naples "Federico II," Italy in 1994 and the Ph.D. degree from the University of Bristol, U.K., in 1998.

In 1997, he was appointed Lecturer in Nonlinear Systems with the Department of Engineering Mathematics of the same University. He has visited the Department of Electrical Engineering, University of Houston, TX, the Department of Applied Mathematics, Universitat Politecnica de Catalunya, Barcelona, Spain, and the Department of Automatic Control, Lund Institute of Technology, Sweden. He has published several papers in international journals. His research interests include the analysis of piecewise smooth systems, applications of nonlinear dynamics to engineering and power electronics, and adaptive control of nonlinear dynamical systems.

In 1997, Dr. di Bernardo was recognized as a Finalist at the Young Author Contest at the Control of Oscillations and Chaos Conference, St. Petersburg, Russia.

Michael Peter Kennedy (S'84–M'91–SM'95–F'98) received the B.E. degree in electronics from the National University of Ireland in 1984 and the M.S. and Ph.D. degrees from the University of California, Berkeley, in 1987 and 1991, respectively, for his contributions to the study of neural networks and nonlinear dynamics.

He worked as a Design Engineer with Philips Electronics, a Postdoctoral Research Engineer with the Electronics Research Laboratory, UC Berkeley, and as a Professeur Invité with the EPFL, Switzerland. He returned to University College Dublin (UCD) in 1992 as a College Lecturer with the Department of Electronic and Electrical Engineering, where he taught electronic circuits, computer-aided circuit analysis, and nonlinear circuits and systems, and directed the undergraduate electronics laboratory. He was appointed Statutory Lecturer at UCD in 1996 and Associate Professor in 1999. Also in 1999, he was appointed Professor and Head of the Department of Microelectronic Engineering at University College Cork. He has published more than 180 articles in the area of nonlinear circuits and systems and has taught courses on nonlinear dynamics and chaos in England, Switzerland, Italy, and Hungary. He has held visiting research positions at the EPFL, AGH Kraków, TU Budapest, and UC Berkeley. His research interests are in the simulation, design, and analysis of nonlinear dynamical systems for applications in communications and signal processing. He is also engaged in research into algorithms for mixed-signal testing.

Dr. Kennedy received the 1991 Best Paper Award from the *International Journal of Circuit Theory and Applications*, the Best Paper Award at the *European Conference on Circuit Theory and Design 1999*, and the Millenium Medal of the IEEE Circuits and Systems Society. He served as an Associate Editor of the IEEE TRANSACTIONS ON CIRCUITS AND SYSTEMS—PART I from 1993 to 1995, as Guest Editor of Special Issues on "Chaos Synchronization and Control" (1997) and "Advances in Nonlinear Electronic Circuits" (1999). He was Chair of the IEEE Technical Committee on Nonlinear Circuits and Systems during 1998–1999 and is currently Associate Editor of the IEEE TRANSACTIONS ON CIRCUITS AND SYSTEMS—PART II. He was elected a Fellow of the IEEE in 1998 "for contributions to the theory of neural networks and nonlinear dynamics, and for leadership in nonlinear circuits research and education."